

A SIMPLE Approach to Provably Reconstruct Ising Model with Global Optimality

Junxian Zhu, Xuanyu Chen, Jin Zhu, Xueqin Wang* and Heping Zhang[†]

University of Science and Technology of China

National University of Singapore, Singapore

Sun Yat-Sen University, Yale University

Abstract

Reconstruction of interaction network between random events is a critical problem arising from statistical physics and politics to sociology, biology, and psychology, and beyond. The Ising model lays the foundation for this reconstruction process, but finding the underlying Ising model from the least amount of observed samples in a computationally efficient manner has been historically challenging for half a century. By using the idea of sparsity learning, we present a approach named SIMPLE that has a dominant sample complexity from theoretical limit. Furthermore, a tuning-free algorithm is developed to give a statistically consistent solution of SIMPLE in polynomial time with high probability. On extensive benchmarked cases, the SIMPLE approach provably reconstructs underlying Ising models with global optimality. The application on the U.S. senators voting in the last six congresses reveals that both the Republicans and Democrats noticeably assemble in each congresses; interestingly, the assembling of Democrats is particularly pronounced in the latest congress.

Keywords: Ising model, best-subset selection, pseudo-likelihood, polynomial time complexity, consistent algorithm

*Wang's research is partially supported by the National Natural Science Foundation of China (12231017), the National Key R&D Program of China (2022YFA1003803), and the National Natural Science Foundation of China (72171216, 71921001, and 71991474).

[†]Zhang's research is partially supported by the U.S. National Institutes of Health (R01HG010171 and R01MH116527) and NSF (DMS-2112711).

1 Introduction

In contemporary applications, Ising model serves as a prevalent tool for characterizing the pairwise interactions between binary variables in a network system. In this network, each node represents a binary variable, the presence of an edge between any two nodes indicates that the corresponding variables have an interaction. Reconstructing the corresponding graph of Ising model is critical to the studies of interaction in a broad spectrum of complex systems in biology, neuroscience, ecology, economics, political science, image analysis (Cocco et al., 2009; Weistuch et al., 2021; Noble et al., 2018; Battiston et al., 2016; Banerjee et al., 2008; Saremi and Sejnowski, 2013).

To be more specific, consider a network with p nodes, it can be parameterized by a p -by- p matrix J with entries J_{ij} being the interaction between nodes i and j . When $J_{ij} = 0$, nodes i and j have no interaction and they are not connected in the network; otherwise, they are neighbors of each other. Under this parameterization, the probability¹ of any observed sample $z = (z_1, \dots, z_p) \in \{-1, 1\}^p$ from the system reads

$$P(z) = \frac{1}{\Phi(J)} \exp \left(\sum_{i \leq j} J_{ij} z_i z_j \right),$$

where $\Phi(J)$ is the partition function that ensures $\sum_{z \in \{-1, 1\}^p} P(z) = 1$. Ising model reconstruction aims to recover J that characterizes variables' interactions via n observed samples $z^{(1)}, \dots, z^{(n)}$ independently sampled from an underlying Ising model. Specifically, in this paper, we focus on this problem when the underlying graph only has a relatively small number of edges, i.e., the vast majority of the J_{ij} 's are exactly zero. This sparsity assumption is reasonable as it gives better interpretability of the model. In the meanwhile, it appears to be a necessary assumption when the dimension p is comparable to or larger than the sample size n (so called the high-dimensional regime). In this scenario, recon-

¹For simplicity, we consider the Ising model with zero external magnetic field.

struction is referred to as recovering both the associating graphical structure and values of J of the underlying Ising model, and the origin of this task dates back to at least 1969 (Kunkin and Frisch, 1969). While many methods have been proposed during the past half century for reconstructing Ising models, finding the most sample efficient estimate in a computationally efficient manner such as in a polynomial time remains an open problem. Given the profound importance of the Ising model, especially in the era of social media, there is an urgent need to solve this open problem.

Reconstructing Ising models by maximizing the likelihood function is considered to be the gold standard, although it is computationally intractable since the evaluation of the partition function $\Phi(J)$ involves the sum of 2^p terms (Nguyen et al., 2017). Many techniques have been developed to approximate the likelihood function. For instance, it is suggested that Monte Carlo methods can be used to approximate the partition function (Geyer, 1994; Miasojedow and Rejchel, 2018), and then the approximating likelihood function is maximized. Note that although this approach is asymptotically exact, it takes an exponential number of runs to achieve a predefined accuracy. Alternative methods that can avoid evaluating the partition function include the naive mean-field approximation and its advanced variants (Chow and Liu, 1968; Kappen and de Borja Rodríguez Ortiz, 1997; Nguyen and Berg, 2012). These variational methods assume that the network is composed of some basic clusters, and when this assumption is met, they give the exact value of the likelihood function. As one increase the size of basic clusters, the methods apply to a broader class of networks, while the computational complexity also shapely grows. However, for networks beyond the applicable class, the effectiveness of such approximations remains un-investigated.

Instead of approximations, surrogates of the likelihood function also have been pro-

posed to sidestep the computational cost. Ravikumar et al. (2010) proposed to nodewise maximize the conditional likelihood. The product of conditionals, commonly referred to as pseudo-likelihood or composite likelihood, is often coupled with various regularizations and widely applied in the literature (Besag, 1975; Höfling and Tibshirani, 2009; Jalali et al., 2011; Xue et al., 2012). In Vuffray et al. (2016), one proposed to use the interaction screening objective (ISO), which is closely related to the exponential loss of the logistic model. These methods are capable for general Ising models and can alleviate the prohibitive computation for their reconstruction. Disadvantages of this strategy include estimation biasness, as well as the subtle steps in tuning hyperparameters and selecting post-inference thresholds for theoretic guarantees (Lokhov et al., 2018). More importantly, we prefer methods that use the fewest samples to perfectly recover the underlying Ising model. However, every aforementioned method requires sample sizes much larger than the necessary sample complexity derived in Santhanam and Wainwright (2012). The best result is the optimality along only a subset of the parameters (Lokhov et al., 2018).

Graphical structure recovery actually resides in the realm of feature selection, for which the predominance of sparse learning approach have been demonstrated in a variety of statistical models (Raskutti et al., 2011; Sara van de Geer and Peter Bühlmann, 2013). Clearly, the sparse learning approach directly address the biasness of the aforementioned regularization based methods. Moreover, the approach may lead to stronger statistical properties, as they usually result in a smaller parameter space to search over. Finally, the development of statistical tools allows us to consider directly solving the sparse learning problem. For some well-studied models like (generalized) linear models, in recent years, statisticians have proposed a number of feasible approximate algorithms that solve the sparse regression under mild conditions (Huang et al., 2018; Zhu et al., 2020; Zhang et al., 2023; Zhu et al., 2022).

However, for Ising models, the potential benefits of the sparse learning approach have not yet been rigorously authenticated, and how to design a feasible algorithm that captures the essence of sparse learning for reconstructing Ising model remains another meaningful problem.

In this paper, we consider a direct but largely-unexplored approach, the sparsity learning, for the reconstruction of Ising models. By using pseudo-likelihood as the objective function, we derive the theoretic sample complexity of the sparse estimator for Ising models. It is lower than that of any existing method, which demonstrates the theoretical advantage of our approach. Building upon this theoretical foundation, we proceed to devise a tractable algorithm for identifying the true graphical structure of an Ising model, with provable computational feasibility and statistical consistency. We also demonstrate that the empirical sample complexity of this polynomial algorithm lies within the globally optimal regime, where the term *global* stands for optimality along all structural parameters that are of interest. Finally, we establish dominance of our proposal over other state-of-the-art methods via simulations under both asymptotic and non-asymptotic regimes, as well as real data analysis.

2 The SIMPLE and its Sample Complexity

In Section 2.1, we describe a sparse learning framework for reconstructing the network associated with the Ising model. Impressively, as we will discuss in Section 2.2, the theoretical support for this framework claims that it has a superior sample complexity.

2.1 Sparse Ising model via pseudo likelihood

We begin by introducing notations for the presentation of our framework. Let J_i be the i -th column of the interaction matrix J , then for each node i in this network, we define logarithmic pseudo likelihood (PL) as

$$\mathcal{L}_n(J_i) := \sum_{r=1}^n \log P(z_i^{(r)} | z_1^{(r)}, \dots, z_{i-1}^{(r)}, z_{i+1}^{(r)}, \dots, z_p^{(r)}).$$

To put it simply, when the interaction between node i and the others is J_i , the PL measures the probability of observing node i 's collected samples given the other nodes' samples. To rephrase, $\mathcal{L}_n(J_i)$ measures the reliability of J_i given the observed data. Having a greater value for $\mathcal{L}_n(J_i)$ indicates that J_i adequately explains the variance of node i . Next, we define the number of neighbors of node i , $\mathcal{N}(J_i) := \#\{J_{ij} \neq 0 \mid j \neq i\}$. Indeed, $\mathcal{N}(J_i)$ naturally characterizes the complexity of the local system of node i .

Our framework is expressed as a compromise between local system accuracy $\mathcal{L}_n(J_i)$ and local system complexity $\mathcal{N}(J_i)$, which is defined as:

$$\hat{J}_i \leftarrow \arg \max_{J_i} \mathcal{L}_n(J_i) \quad \text{s.t. } \mathcal{N}(J_i) \leq d \quad (\text{for } i = 1, \dots, p) \quad (1)$$

in which d is an integer specifying the maximum acceptable local complexity. The term for this approach that we've coined is sparse Ising model via PL (SIMPLE). Concatenating $(\hat{J}_1, \dots, \hat{J}_p)$, the solutions of (1), and then performing an additional matrix symmetrization step completes the reconstruction of an Ising model.

Remark 1 *The advantage of SIMPLE is two-folded. First, it meets the need for reconstructing networks by selecting the neighbors of each node. Once neighbors of every node are correctly found, the network structure must be identical to the true one. Particularly, the local system complexity constraint conducts the selection of neighbors straightforwardly,*

which is the key reason for the superiority of SIMPLE. In contrast, the other indirect constraints would need higher sample complexity to implicitly select the neighbors. Second, it exploits the PL $\hat{J}_i (i = 1, \dots, p)$ as surrogate of the computationally intractable likelihood function. Actually, it has an explicit expression:

$$\mathcal{L}_n(J_i) = - \sum_{r=1}^n \log \left\{ \exp \left(- 2 \sum_{j:j \neq i} J_{ij} z_i^{(r)} z_j^{(r)} \right) + 1 \right\},$$

and computing PL has an $O(np)$ time complexity and thus can be quickly computed.

2.2 Sample complexity of SIMPLE

For the reconstruction of Ising models, sample complexity refers to the minimum sample size such that, with a high probability, the estimator can recover any underlying true graph. Here, we assume the underlying distribution P_J that associates with interaction matrix J belongs to the following family of distributions, as in the related previous works (Santhanam and Wainwright, 2012; Lokhov et al., 2018; Dedieu et al., 2021)

Definition 1 (Santhanam and Wainwright (2012)) *For a suitable pair of positive constant (λ, γ) , we define $\mathcal{G}_{p,d}(\lambda, \gamma)$ as the family of distributions $P_{J(G)}$ such that:*

- (i) *The underlying graph $G \in \mathcal{G}_{p,d}$, where $\mathcal{G}_{p,d}$ is the class of graphs with p nodes and bounded degree d ;*
- (ii) *The parameter matrix $J(G)$ corresponds with the graph structure G , i.e., $J_{ij} \neq 0$ is equivalent to $(i, j) \in E(G)$;*
- (iii) *Define the minimum and maximum signal strength of J as $\lambda := \min_{(i,j) \in E} |J_{ij}|$ and $\gamma(J) := \max_{i \in V} \|J_i\|_1$ respectively. They satisfies the following bounds: $\lambda(J) \geq \lambda$, and $\gamma(J) \leq \gamma$.*

Remark 2 *For $\mathcal{G}_{p,d}(\lambda, \gamma)$, structural parameters λ, γ, d, p are of primary interest when investigating the sample complexity. Santhanam and Wainwright (2012) indicates several*

crucial features of the optimal sample complexity n_{opt} on its dependencies on (λ, γ, d, p) : $n_{opt} \propto \ln p$, $n_{opt} \propto \frac{1}{\lambda^2}$, $n_{opt} \propto d^r$ and $n_{opt} \propto e^{c\gamma}$ with the precise values of constants $r \in [1, 2]$ and $c \in [1, 4]$ remaining unknown. These four dependencies with arbitrary $r \in [1, 2]$ and $c \in [1, 4]$ are referred to as the globally optimal regime, and estimators satisfying all of them are called globally optimal.

We define some notations for our following analysis of SIMPLE. For a given graph $G \in \mathcal{G}_{p,d}$, let $J_{\lambda,\gamma}(G)$ be the family of symmetric parameter matrices corresponding with the graph structure G and satisfying that for arbitrary $J \in J_{\lambda,\gamma}(G)$, we have distribution $P_J \in \mathcal{G}_{p,d}(\lambda, \gamma)$. Denote the p nodes by $V := \{1, \dots, p\}$. For any pair $G = (V, E) \in \mathcal{G}_{p,d}$ and $J \in J_{\lambda,\gamma}(G)$, define $G_i = (V, E_i)$ as the neighborhood of node i in G , where $E_i := \{(i, j) \mid (i, j) \in E, j \in V\}$. The corresponding parameter vector is denoted by J_i . The sets of all possibilities of G_i and J_i are denoted by $\mathcal{G}_{p,d,i}$ and $J_{\lambda,\gamma,i}(G_i) \subseteq \mathbb{R}^{p-1}$ respectively. Stacking the observations into a sample matrix $\mathbf{Z} \in \{-1, +1\}^{n \times p}$ with $(z^{(r)})^\top$ being its r th row.

For each node $i \in V$, SIMPLE firstly maximizes PL over all possible parameters of the neighborhood, and secondly, it searches for the graphical structure that maximizes the values obtained in the first step; and thus, the two step procedure is summarized as:

$$(V, \hat{E}_i) := \arg \max_{G_i \in \mathcal{G}_{p,d,i}} \max_{J_i \in J_{\lambda,\gamma,i}(G_i)} \mathcal{L}_n(J_i),$$

Combine nodewise results, the estimator of SIMPLE is expressed as $\phi^*(\mathbf{Z}) := (V, \bigcup_{i=1}^p \hat{E}_i)$.

Allowing the quadruple (λ, γ, d, p) to scale with the sample size n , the following theorem gives the theoretic sample complexity of SIMPLE to successfully recover the underlying graph structure.

Theorem 1 Assume that $\frac{\gamma}{e^{3\gamma}} \sinh^2\left(\frac{\lambda}{2}\right) < 1$ and $e^{2\gamma} \geq 3$. For arbitrary $G^* = (V, E^*) \in \mathcal{G}_{p,d}$ and $J^* \in J_{\lambda,\gamma}(G^*)$, suppose each row of \mathbf{Z} are i.i.d drawn from $P_{J^*}(Z)$. For any

constant $\varepsilon \in (0, 1)$, if the sample size n satisfies

$$n \geq n^* = \frac{8e^{5\gamma}}{\gamma \sinh^2(\lambda/2)} \left(3d \ln p + d \ln \left(1 + \frac{24de^{5\gamma}}{\sinh^2(\lambda/2)} \right) + \ln \frac{1}{\varepsilon} \right),$$

then we have $P_{J^*}(\phi^*(\mathbf{Z}) \neq G^*) \leq \varepsilon$.

Corollary 1 can be presented in a more concise style:

Corollary 1 *Under the same terminologies and conditions of Theorem 1, additionally assume that $\lambda < 1$ and $\gamma = O(\ln \frac{1}{\lambda})$, then for any constant $\varepsilon \in (0, 1)$, if the sample size n satisfies*

$$n \geq n^* = O \left(\frac{d}{\lambda^2} e^{5\gamma} \ln \frac{p}{\varepsilon} \right),$$

with probability at least $1 - \varepsilon$, SIMPLE recovers the underlying structure.

This result is aligned with the information-theoretic lower bound on p , λ , d and nearly optimal on γ . Along every axis of (λ, γ, d, p) , it matches or improves the theoretic sample complexities of all existing algorithms. Note that all four assumptions made in Corollary 1, $\frac{\gamma}{e^{3\gamma}} \sinh^2(\frac{\lambda}{2}) < 1$, $e^{2\gamma} \geq 3$, $\lambda < 1$ and $\gamma = O(\ln \frac{1}{\lambda})$ are all used only for simplifying expressions. They are satisfied in most cases we are interested in. For example, as n increases, p , d and γ increase while λ tends to 0, the four assumptions would hold.

The SIMPLE's sample complexity scales linearly in the maximum number of neighbors d , while other existing methods have theoretic sample complexities growing quadratically in d . This is particularly important in practice because systems with highly connected nodes (e.g., scale-free networks (Barabási, 2009)) are ubiquitous in fields like neuroscience and sociology (Grabowski, 2009; Marinazzo et al., 2014). In these cases, SIMPLE uses the fewest samples to perfectly recover these highly connected nodes. Most notably, our method proves a conjecture in Santhanam and Wainwright (2012) as its sample complexity scale linearly with d . We know that the optimal sample complexity scales with d^c , where

$c \in [1, 2]$ is an unknown precise number conjectured to be 1, according to the work of Santhanam and Wainwright (2012). By providing support for the claim that $r = 1$ for the SIMPLE, our finding verifies the truth of this supposition.

For the maximum of the cumulative interaction magnitudes γ , the SIMPLE also has the state-of-the-art theoretic sample dependency. In the case of large γ , the underlying Ising model is low-temperature, which is shown to be challenging to reconstruct (Montanari and Pereira, 2009; Nguyen and Berg, 2012) and attracts keen attention from researchers (Decelle and Ricci-Tersenghi, 2014; Nguyen and Berg, 2012). Roughly speaking, the difficulty arises since in this case, most samples we collect would be of the network’s ground states. The sample size needed to include a sufficient number of non-trivial samples grows exponentially as γ increases. Therefore, SIMPLE has a greater potential for widespread use because it uses significantly fewer samples to reconstruct a low-temperature Ising model than existing approaches. Examples illustrating this advantage are provided in Figure 2. Specifically, the SIMPLE’s empirical sample complexity is lower than the other methods, one of which is an γ -optimal method Lokhov et al. (2018).

Last but not least, our proposed sample complexity for a given number of nodes p and the minimum interaction λ is a perfect match to the optimal sample complexity given by Santhanam and Wainwright (2012), i.e., it is proportional to $\log p$ and λ^{-2} . For high-dimensional binary variables, where p can scale exponentially with n , the former result is significant. The last implication means that no alternative structure recovery approach can use fewer samples than our proposal when the signal-to-noise ratio is relatively low.

The reason why the SIMPLE outperforms LASSO-type approaches in terms of sample complexity can be intuitively understood as follows. SIMPLE’s candidate solution space is contained within that of Lasso-type estimators. Therefore, the SIMPLE narrows the search

space for the correct Ising model, which naturally results in a reduced number of samples needed compared to the Lasso-type approaches.

3 Algorithm and its Properties

The time complexity grows sharply with p when using enumeration to solve SIMPLE. Therefore, to enhance the practical usability of SIMPLE, we have presented an iterative algorithm in Section 3.1. The subsequent Section 3.2 will exhibit both the computational and statistical properties of this algorithm.

3.1 Algorithmic description

Our algorithm mainly consists of three nested loops, as summarized in Algorithm 1. In the innermost loop, our objective is to find the neighborhood of each fixed node i when the number of neighbors d is fixed. Regarding the middle loop, its purpose is to select the best neighborhood size d for each fixed node i . Consequently, the middle loop returns the neighbor set for the fixed node i . Finally, the outer loop simply concatenates the results of the middle loop to reconstruct the entire graph. Below, we will provide more details about the inner and middle loops.

The inner loop employs the splicing technique proposed by Zhu et al. (2020). The idea behind the *splicing* technique is simple to grasp. For a given node i , if we have a current best guess for its neighbors' topology, we can improve the quality of our estimate by including the nodes that are important to improve $\mathcal{L}_n(J_i)$ and eliminating the ones that have less importance. Below, we provide a formal characterization of the importance. Suppose the neighborhood $\mathcal{A} \subseteq V \setminus \{i\}$ and the interaction $\hat{J}_i = \arg \max_{\text{supp}(J_i)=\mathcal{A}} \mathcal{L}_n(J_i)$ are our current guess, we introduce two types of importance: (i) the *backward importance* \hat{J}_{ij}^2 and

(ii) the *forward importance* $\hat{\eta}_j^2$ where $\hat{\eta}_j = \nabla_j \mathcal{L}_n(\hat{J}_i)$.

Remark 3 *Backward importance can be interpreted as the price we pay for removing node $j \in \mathcal{A}$ from the current neighborhood \mathcal{A} , as one can show $C\hat{J}_{ij}^2 \approx \mathcal{L}_n(\hat{J}_i) - \mathcal{L}_n(\hat{J}_i|_{\mathcal{A} \setminus \{j\}})$ where C is some universal constant and $\hat{J}_i|_{\mathcal{A} \setminus \{j\}}$ is obtained by setting the j th entry of \hat{J}_i to zero. Analogously, forward importance can be interpreted as the gain of including node $j \in \mathcal{A}^c$ into \mathcal{A} due to $C'\hat{\eta}_j^2 \approx \max_{t \in \mathbb{R}^{p-1}, \text{supp}(t)=\{j\}} \mathcal{L}_n(\hat{J}_i + t) - \mathcal{L}_n(\hat{J}_i)$, where C' is some universal constant.*

Furthermore, for any given $s \leq d$, define

$$\begin{aligned} \mathcal{S}_{s,1} &= \{j \in \mathcal{A} : \hat{J}_{ij}^2 \text{ is one of the last } s \text{ backward importance}\}, \\ \mathcal{S}_{s,2} &= \{j \in \mathcal{A}^c : \hat{\eta}_j^2 \text{ is one of the top } s \text{ forward importance}\}. \end{aligned} \tag{2}$$

Then, we splice \mathcal{A} to create a new neighborhood structure by letting $\tilde{\mathcal{A}} = (\mathcal{A} \setminus \mathcal{S}_{s,1}) \cup \mathcal{S}_{s,2}$. Setting $\tilde{J}_i = \arg \max_{\text{supp}(J_i)=\tilde{\mathcal{A}}} \mathcal{L}_n(J_i)$, then $\tilde{\mathcal{A}}$ is deemed to be a better guess than \mathcal{A} if $\mathcal{L}(\tilde{J}_i) > \mathcal{L}_n(\hat{J}_i)$, then we shall update (\mathcal{A}, \hat{J}_i) with $(\tilde{\mathcal{A}}, \tilde{J}_i)$. The splicing technique is iteratively applied until the inner loop cannot find a better neighbor set.

The main idea of middle loop is to determine the optimal neighbor size d for the fixed node $i \in V$ that guarantees a good balance between the system's accuracy and its complexity. Specifically, given the interaction of the i -th node returned by the inner loop under the neighbor size d_i , denoted as \hat{J}_{i,d_i} , we assess \hat{J}_{i,d_i} with *generalized information criterion* (GIC)

$$\text{GIC}(\hat{J}_{i,d_i}) := \mathcal{L}_n(\hat{J}_{i,d_i}) - d_i \log p \log \log n,$$

where the term $d_i \log p \log \log n$ encourages using fewer neighbors to explain the data so as to prevent overfitting caused by the incorrect inclusion of neighbors that weakly interact with node i . To get the optimal number of neighbors, the middle loop selects a d_i from $\{0, 1, \dots, p-1\}$ that maximizes $\text{GIC}(\hat{J}_{i,d_i})$.

Remark 4 *Two features of the algorithm make it even more practically interesting. First, the algorithm exploits the fact that the number of unknown best neighbors from which to choose is discrete. Selecting a discrete neighbor’s number is more interpretable than choosing a continuous tuning parameter as the approaches in the literature. It is even more useful when there is a priori knowledge or expertise about the actual number of neighbors. For LASSO-type methods, this information has to be leveraged in a post-hoc manner.*

Furthermore, during iterations, the proposed algorithm estimates the interactions between nodes without shrinking them, leading to an unbiased estimate of the interactions. Consequently, our algorithm gives more accurate estimation of the interactions, especially in the small-sample regime, which can be witnessed by the smallest interaction estimation errors in Figure 3.

Finally, in most cases, it is also challenging to know a priori what the smallest interaction λ is. Notably, this procedure implicitly determines λ in a data-driven way and gives a proper estimation for complexity.

We close this section with a discussion of the input parameters of Algorithm 1.

- The threshold σ_d is introduced to reduce unnecessary splicing steps, when the model size d is underestimated or the algorithm has already recovered the true graphical structure. Condition (C3) for the theoretical properties provide a reference for the determination of σ_d from the asymptotic point of view. In our implementation, we set $\sigma_d = 0.01 \frac{d \log p \log \log n}{n}$.
- s_{\max} is a positive constant that controls the maximum splicing size. In our implementation, we fix it as $s_{\max} = d_{\max}$ to guarantee the statistical and computational properties.

Algorithm 1

Input: Splicing threshold σ_d , maximal splicing size s_{\max} , maximum degree d_{\max} , graphical threshold τ .

```
1: for  $i = 1, \dots, p$  do                                 $\triangleright$  Outer loop: nodewise sparse learning
2:    $\hat{J}_{i,0} \leftarrow \mathbf{0}, \eta_{i,0} \leftarrow \nabla \mathcal{L}(\hat{J}_{i,0})$ .
3:   for  $d = 1, \dots, d_{\max}$  do                         $\triangleright$  Middle loop: searching the optimal  $d$  with GIC
4:      $k \leftarrow -1, \mathcal{A}^0 \leftarrow \text{supp}(\hat{J}_{i,d-1}) \cup \{\arg \max_i (\eta_{i,d-1})^2\}$ .  $\triangleright$  Warm-start initialization
5:     repeat                                            $\triangleright$  Inner loop: iteratively employing the splicing
6:        $k \leftarrow k + 1, J_i^k \leftarrow \arg \max_{\text{supp}(J_i) = \mathcal{A}^k} \mathcal{L}_n(J_i), \eta^k \leftarrow \nabla \mathcal{L}_n(J_i^k)|_{(\mathcal{A}^k)^c}$ .
7:       for  $s = 1, \dots, \min\{d, s_{\max}\}$  do
8:         Compute  $\mathcal{S}_{s,1}^k$  and  $\mathcal{S}_{s,2}^k$  according to (2).
9:          $\tilde{\mathcal{A}}^k \leftarrow (\mathcal{A}^k \setminus \mathcal{S}_{s,1}^k) \cup \mathcal{S}_{s,2}^k$  and solve  $\tilde{J}_i^k = \arg \max_{\text{supp}(J_i) = \tilde{\mathcal{A}}^k} \mathcal{L}_n(J_i)$ .
10:        if  $\mathcal{L}_n(\tilde{J}_i^k) - \mathcal{L}_n(J_i^k) > \sigma_d$ , then
11:           $(\mathcal{A}^{k+1}, J_i^{k+1}, \eta^{k+1}) \leftarrow (\tilde{\mathcal{A}}^k, \tilde{J}_i^k, \nabla \mathcal{L}_n(\tilde{J}_i^k)|_{(\mathcal{A}^k)^c})$ 
12:        end if
13:      end for
14:    until  $\mathcal{A}^k = \mathcal{A}^{k-1}$ 
15:     $\hat{J}_{i,d} \leftarrow J_i^k, \eta_{i,d} \leftarrow \eta^k$ .  $\triangleright$  Solution of Inner Loop
16:  end for
17:   $\hat{d} = \arg \max_{1 \leq d \leq d_{\max}} \text{GIC}(\hat{J}_{i,d}), \hat{J}_i \leftarrow \hat{J}_{i,\hat{d}}$ .  $\triangleright$  Solution of Middle Loop
18: end for
19: for  $i, j = 1, \dots, p$  do
20:    $\hat{J}_{ij} \leftarrow \frac{1}{2}(\hat{J}_{ij} + \hat{J}_{ji}) \mathbb{I}(\frac{1}{2}|\hat{J}_{ij} + \hat{J}_{ji}| \geq \tau)$   $\triangleright$  Threshold the solution of Outer Loop
21: end for
```

Output: \hat{J} .

- To incorporate prior information on d , we can set $d_{\max} = d$. When no knowledge on d is available, the theoretic analysis for Algorithm 1 suggests setting $d_{\max} = \lceil \frac{n}{\log p \log \log n} \rceil$.
- The graphical thresholding τ helps reduce false recoveries when the minimum signal λ is known. In such cases, we suggest $\tau = \lambda/2$ as in Lokhov et al. (2018); otherwise, simply set $\tau = 0$.

3.2 Theoretical Guarantees on the Algorithm

We first introduce the necessary notations and conditions.

(C1) For given $i \in V$ and d_{\max} , define the random vector set

$$\Lambda_{i,d}(\mathbf{Z}) := \left\{ \hat{J}_i(\mathbf{Z}) : \hat{J}_i(\mathbf{Z}) = \arg \max_{\text{supp}(J_i)=\mathcal{A}} \mathcal{L}_n(J_i), \forall \mathcal{A} \text{ s.t. } |\mathcal{A}| \leq d \right\} \bigcup \left\{ J_i^* \right\},$$

there exists a universal constant $c \geq 1$ such that

$$P \left\{ \max_{i \in V} \max_{J_i \in \Lambda_{i,d_{\max}}(\mathbf{Z})} \|J_i\|_1 \leq c\gamma \right\} < \varepsilon_0 = o(1).$$

Remark 5 Condition (C1) places a restriction on the magnitude of SIMPLE across all possible models, since the curvature of PL may vanish at some points far away from the origin. In the context of generalized linear models, similar conditions with the same purpose are commonly encountered and are intended to avoid infinitely large or small variance of y_i , as well as ensure the existence of the Fisher information for statistical inference (Rigollet, 2012; Fan and Tang, 2013).

For arbitrary support size d , we define $B_d := \max_{\mathcal{A}: |\mathcal{A}| \leq d} \lambda_{\max}(\mathbb{E}[Z_{\mathcal{A}} Z_{\mathcal{A}}^{\top}])$, $b_d := \min_{\mathcal{A}: |\mathcal{A}| \leq d} \lambda_{\min}(\mathbb{E}[Z_{\mathcal{A}} Z_{\mathcal{A}}^{\top}])$, and $\mu_d := \max_{\mathcal{A}, \mathcal{B}: |\mathcal{A}| \leq d, |\mathcal{B}| \leq d, \mathcal{A} \cap \mathcal{B} = \emptyset} \sigma_{\max}(\mathbb{E}[Z_{\mathcal{A}} Z_{\mathcal{B}}^{\top}])$.

(C2) Denote $\gamma_d := \frac{C_1(d, \gamma, \Delta)}{(1-\Delta)C_2(d, \gamma, \Delta)}$ where

$$C_1(d, \gamma, \Delta) = \frac{4(1+\Delta)^7 \mu_d^2}{(1-\Delta)^6 e^{-4c\gamma} b_d^2} \left(\frac{B_d}{2} + \frac{\mu_d^2}{e^{-2c\gamma} b_d} + \frac{B_d \mu_d^2}{2e^{-4c\gamma} b_d^2} \right) \left(2 + \frac{2\mu_d}{e^{-2c\gamma} b_d} + \frac{\mu_d^2}{e^{-4c\gamma} b_d^2} \right),$$

$$C_2(d, \gamma, \Delta) = \frac{(1-\Delta)}{2} e^{-2c\gamma} b_d - \frac{(1+\Delta)^3}{(1-\Delta)^2} \left(\frac{\mu_d^2}{e^{-2c\gamma} b_d} + \frac{B_d \mu_d^2}{2e^{-4c\gamma} b_d^2} \right),$$

Suppose that $\exists \Delta \in (0, 1)$, such that $0 \leq \gamma_{d_{\max}} < 1$.

Remark 6 Condition (C2) is a technical requirement. The quantities B_d , b_d and μ_d are widely used in modeling high-dimensional data. They restrict the correlation among a small number of variables and, in turn, guarantee the identifiability of the true active set. B_d and $e^{-2c\gamma} b_d$ are actually upper and lower bounds for the spectrum of the Hessian matrix over supports with a restricted cardinality. Condition (C2) is satisfied when they are closed enough and μ_d is sufficiently small. Specifically, in an asymptotic point of view, in order to guarantee that $C_2(d, \gamma, \Delta) > 0$, μ_d is required to decay exponentially with γ . Intuitively, this requires PL to be both smooth and convex enough, and column vectors of the design matrix are nearly orthogonal. In particular, this condition holds trivially if the design matrix has orthogonal columns.

(C3) $\sigma_d = \Theta\left(\frac{d \log p \log \log n}{n}\right)$ for any $1 \leq d \leq d_{\max}$.

Remark 7 Conditions (C3) can be decomposed into $\sigma_d = O\left(\frac{d \log p \log \log n}{n}\right)$ and $\sigma_d = \Omega\left(\frac{d \log p \log \log n}{n}\right)$. The former is designed to prevent σ_d from becoming too large, allowing for necessary splicing steps, while the latter aims to reduce unnecessary iterations.

We now present the statistical guarantee of Algorithm 1. The following theorem asserts that the solution of the middle loop consistently identifies the underlying neighbors with high probability.

Theorem 2 (Consistency of Nodewise Neighbor Selection) *Assume Conditions (C1)-(C3) hold and the support size $d^* := |\text{supp}(J_i^*)| \leq d_{\max}$. Denote $\hat{J}_{i,\hat{d}}$ as the j -th column of matrix \hat{J} outputted by Algorithm 1 and $\hat{\mathcal{A}}_{\hat{d}} = \text{supp}(\hat{J}_{i,\hat{d}})$. Then there exists a universal constant $K > 0$ such that, if*

$$n > \max \left\{ \exp \left\{ \exp \left[(1 + \Delta) K e^{4\gamma} \left(1 + \frac{\delta}{d^*} \right) \right] \right\}, \right. \quad (3)$$

$$\left. \frac{\kappa d_{\max} \log p}{(1 - \gamma_{d_{\max}})(1 - \Delta) C_2(d_{\max}, \gamma, \Delta) \lambda^2} \log \left[\frac{\kappa d_{\max} \log p}{(1 - \gamma_{d_{\max}})(1 - \Delta) C_2(d_{\max}, \gamma, \Delta) \lambda^2} \right] \right\},$$

then the true active set is selected with high probability:

$$P(\hat{\mathcal{A}}_{i,\hat{d}} = \text{supp}(J_i^*)) \geq 1 - \varepsilon_0 - \varepsilon_1(d_{\max}) - \varepsilon_2(d_{\max}) - \varepsilon_3(d_{\max}) - \varepsilon'_4(d_{\max}) - d_{\max} p^{-\delta}.$$

Here $\varepsilon_1(d) = 2p^2 \exp \left\{ -\frac{n\Delta^2 B_d^2}{2d^2} \right\}$, $\varepsilon_2(d) = 2p^2 \exp \left\{ -\frac{n\Delta^2 \mu_d^2}{2d^2} \right\}$, $\varepsilon_3(d) = 2p^2 \exp \left\{ -\frac{n\Delta^2 b_d^2}{2d^2} \right\}$ and $\varepsilon_4(d) = 2p \exp \left\{ -\frac{n\lambda^2 t^2(d, \gamma, \Delta)}{8d} \right\}$, $\delta > 0$ is an arbitrary constant, and $\varepsilon'_4(d) = 2p \exp \left\{ -\frac{nt'(d, \gamma, \Delta, \lambda, (\log p/n)^{\frac{1}{3}})^2}{8d} \right\}$ where $t(d, \gamma, \Delta)$ and $t'(d, \gamma, \Delta, \lambda, (\log p/n)^{\frac{1}{3}})$ are constants whose explicit forms are provided in the supplementary material.

Applying the union bound, it is straightforward to obtain the following corollary, which ensures that Algorithm 1 consistently reconstructs the whole graph.

Corollary 2 (Consistency of Structural Recovery for Ising models) *Under the same conditions and notations in Theorem 2, then with probability at least $1 - \varepsilon_0 - \varepsilon_1(d_{\max}) - \varepsilon_2(d_{\max}) - \varepsilon_3(d_{\max}) - p\varepsilon'_4(d_{\max}) - d_{\max} p^{1-\delta}$, Algorithm 1 will select the true active set, i.e.,*

$$\text{supp}(\hat{J}) = \text{supp}(J^*).$$

The next theorem claims that, in a high probability sense, Algorithm 1 has a polynomial time complexity.

Theorem 3 *Assume Conditions (C1)-(C3) hold and Algorithm 1 successfully recover the true graphical structure $\text{supp}(\hat{J}) = \text{supp}(J^*)$ (by Corollary 2, this event is true with a large probability for sufficiently large sample size n). Then the computational complexity of Algorithm 1 for a given $d_{\max} \geq \max_{i \in V} |\text{supp}(J_i^*)|$ is*

$$O\left(\left(\frac{d_{\max}}{1 - \gamma_{d_{\max}}} \ln \frac{n\gamma}{\min_{i \in V} |\text{supp}(J_i^*)| \log p \log \log n} + \frac{n\gamma}{\log p \log \log n}\right)(s_{\max} p n d_{\max} + s_{\max} p^2)\right).$$

We claim that the computational complexity of Algorithm 1 scale as a polynomial in (n, p, d) . In other words, under certain conditions, our algorithm solves the intractable problem of learning sparse Ising model in a polynomial time. To see this, we only need to verify that (B_d, μ_d, b_d) can be selected such that $\frac{1}{1 - \gamma_d} = \frac{(1 - \Delta)C_2}{(1 - \Delta)C_2 - C_1}$ scales at most polynomially with (n, p, d) . This is true since $\lambda_{\max}(\mathbb{E}[Z_{\mathcal{A}} Z_{\mathcal{A}}^{\top}]) \leq d$, $\sigma_{\max}(\mathbb{E}[Z_{\mathcal{A}} Z_{\mathcal{B}}^{\top}]) \leq d$, and $\lambda_{\min}(\mathbb{E}[Z_{\mathcal{A}} Z_{\mathcal{A}}^{\top}]) \geq \frac{e^{-2\gamma}}{d+1}$ where the last inequality is also presented in Lemma 7 of Vuffray et al. (2016). Note that the complexity grows exponentially fast as γ increases, which is aligned with our expectation since the complexity is derived for the case that our algorithm successfully recovers the graphical structure, which, in turn, requires a sample size n to scale exponentially with γ .

4 Simulation studies

The simulation studies are divided into three part. The first part would like to numerical certify SIMPLE has a superiority on empirical sample complexity with respect to d and γ (see Section 4.1). And the second part presented in Section 4.2 is mainly interested in another practice scenario where the number of parameters are comparable or even larger than n , so called high-dimensional regime. The section is closed with numerical experiments on computation performance.

4.1 Numerical advantages on sample complexity

In this part, we leverage the empirical sample complexity n_{emp} to evaluate and compare methods. Roughly speaking, n_{emp} is the empirical counterpart of n^* , recording the minimal numerical sample size that exactly recovers the underlying graphical structure. Its detailed definition is deferred to the supplementary material.

4.1.1 Experiments on d

We first investigate n_{emp} with respect to d to illustrate the efficacy of SIMPLE. The random regular graph (RRG) topology is used in this investigation because it allows the generation of a network of any degree $d < p$ when p, λ, γ are all fixed. To be more specific, to disentangle the effects of d from λ and γ , we force each node having exactly one neighbor with interaction λ and the other interaction being β such that $\gamma = (d - 1)\beta + \lambda$ is a fixed constant.

Figure 1 provides a graphical representation of the corresponding Ising model in its lower right corner. A linear relationship between n_{emp} and d appears to exist in SIMPLE (see Figure 1). This supports the $O(d)$ lower bound on d obtained from our theoretical analysis of the SIMPLE estimator. For the sake of comparison, we also include the LASSO-regularized pseudo-likelihood estimator (RPLE) in this analysis. As can be seen in Figure 1, the slope of the blue line is less steep than that of the red line, indicating that our approach is more sample-efficient than RPLe, as the rate of growth of the empirical sample size for SIMPLE is lower than that for RPLe.

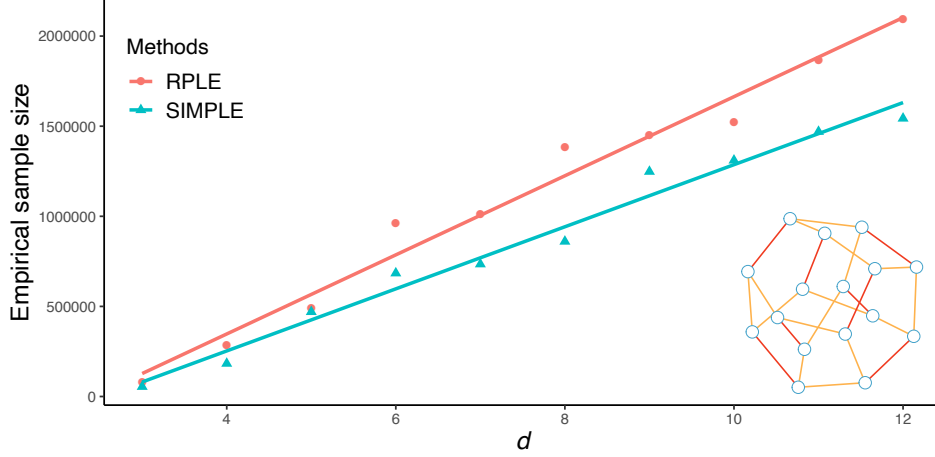


Figure 1: The maximum degree d (x -axis) versus empirical sample size (y -axis) scatterplot under the ferromagnetic RRGs. The network for the $d = 3$ case is presented in the right-bottom corner. The ferromagnetic RRG whose couplings equal to β and λ are colored in orange and red, respectively. The two straight lines are characterized by equations $y = a + bx$, where the coefficients a, b are estimated by linear regression.

4.1.2 Experiments on γ

Here, we empirically achieve the scale of n_{emp} w.r.t. γ across a variety of graphical topologies and interaction patterns via a large set of numerical tests. We take into account five benchmarked distinct Ising models considered in Lokhov et al. (2018). These Ising models cover two reference topologies including RRGs and a periodic-boundary square lattice (PBSL). The two topologies avoid the instability caused by the heterogeneity of nodes to make it simpler to extract the proper scaling with regard to γ . The two sorts of interactions are considered: (i) $J_{ij} > 0$ and (ii) $J_{ij} \in \mathbb{R}$, where all interaction magnitudes $|J_{ij}|$ are set to a positive value β except for the weakest signal λ . It is necessary to fix one coupling in cases (i) to λ and $-\lambda$, respectively, and fix two couplings in cases (ii) to λ and $-\lambda$ in order to separate the effects of λ and γ . The combination of two topologies and two interaction types result in four Ising models. The remain one Ising model is a PBSL with interaction

(i) but one of interaction is weakly negative, which is consider as a hard model for learning graphical structure (Lokhov et al., 2018).

For comparison, a regularized interaction screening estimators (RISE) and its variant, logRISE, are also included in this analysis, where logRISE is a γ -optimal estimator (Lokhov et al., 2018). From Figure 2, the n_{emp} of four methods grows exponentially with regard to γ . It's clear that the SIMPLE has the finest scaling property with respect to γ because its growth rate is the lowest of all these approaches across all five Ising models. Even in its worst case, the empirical scaling of SIMPLE (i.e., $\exp\{3.5\}$ on PBSL with interaction (i)) is still in the optimal range with respect to the information-theoretic prediction. According to Lokhov et al. (2018), a scaling factor of 3.9 for logRISE places it in the γ -optimal regime, while the RISE Ising model estimator comes in at number three among the four methods under comparison.

4.2 High-dimensional regime

To compare the estimation accuracy of different methods in this regime, we consider metrics from two aspects, one focuses on structure recovery and the other on parameter estimation. We measure the accuracy of structure recovery by true positive rate (TPR), false positive rate (FPR) and Matthews correlation coefficient (MCC), which are defined as

$$\begin{aligned} \text{TPR} &= \frac{\text{TP}}{\text{TP} + \text{FN}}, \quad \text{FPR} = \frac{\text{FP}}{\text{TN} + \text{FP}}, \\ \text{MCC} &= \frac{\text{TP} \times \text{TN} - \text{FP} \times \text{FN}}{\sqrt{(\text{TP} + \text{FP})(\text{TP} + \text{FN})(\text{TN} + \text{FP})(\text{TN} + \text{FN})}}, \end{aligned}$$

where TP, TN, FP and FN refer to

$$\begin{aligned} \text{TP} &= \left| \left\{ (i, j) \mid \hat{J}_{ij} \neq 0 \cap J_{ij}^* \neq 0 \right\} \right|, \quad \text{TN} = \left| \left\{ (i, j) \mid \hat{J}_{ij} = 0 \cap J_{ij}^* = 0 \right\} \right|, \\ \text{FP} &= \left| \left\{ (i, j) \mid \hat{J}_{ij} \neq 0 \cap J_{ij}^* = 0 \right\} \right|, \quad \text{FN} = \left| \left\{ (i, j) \mid J_{ij} = 0 \cap \hat{J}_{ij} \neq 0 \right\} \right|. \end{aligned}$$

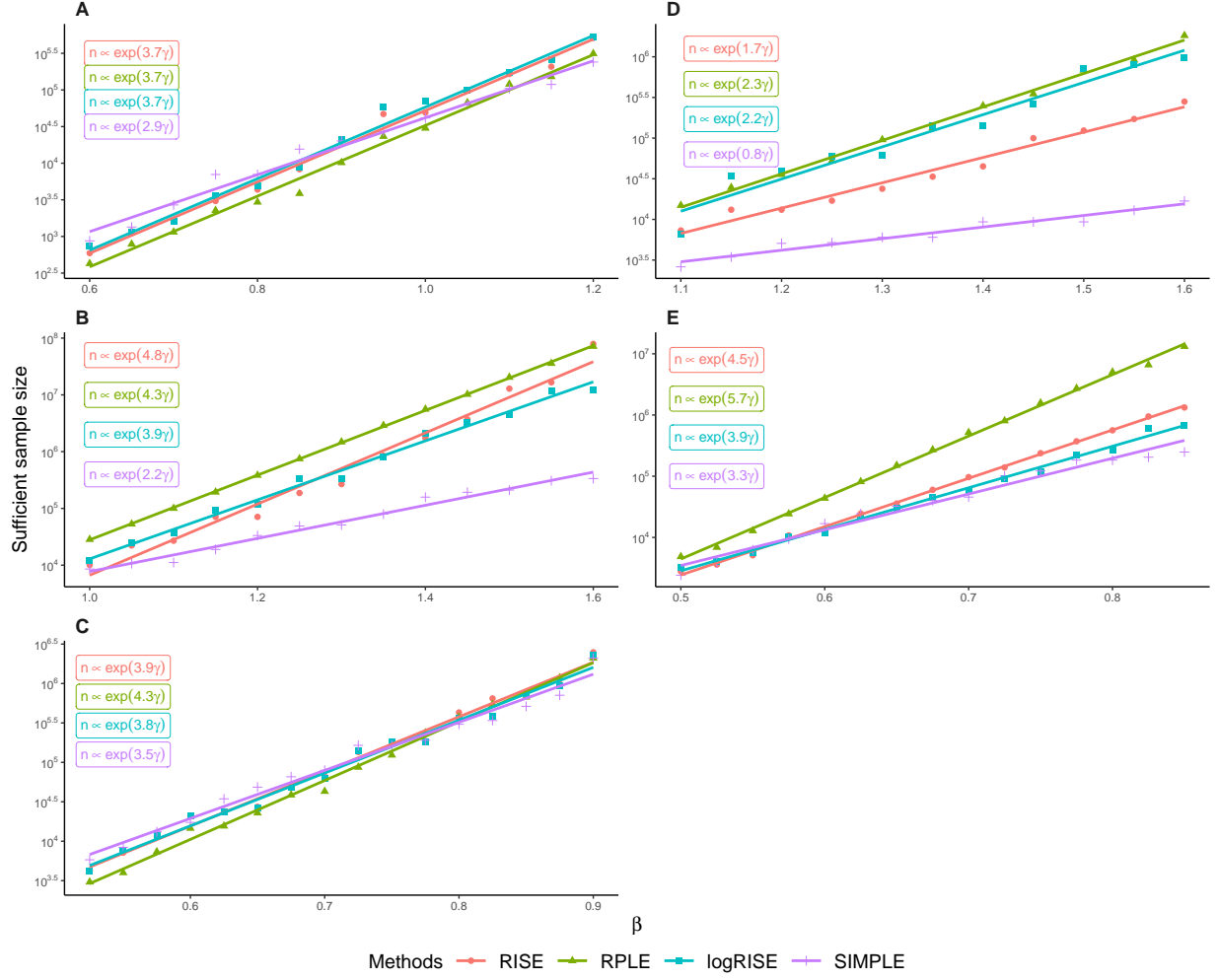


Figure 2: Interactions β (x -axis) versus empirical sample size (\log_{10} -transformed y -axis) scatterplot in six types of Ising models presented in each panel. A method with the smallest slope is the best one; otherwise, the worst. The left panels and right panels correspond to RRGs and PBSLs. The upper, middle, and bottom panels correspond to interaction types (i), (ii), and (iii), respectively. The top-left corner of each panel presents the exponent scaling b of four methods, which are given by estimating the coefficients of linear models $\log(n_{\text{emp}}) = a + b(d\beta)$, where $d = 3$ for RRGs and $d = 4$ for PBSLs.

In terms of interaction estimations, mean square error (MSE) between the estimated and truth is a widely adopted measure for the assessment of parameter accuracy. It is defined as $\text{MSE}(J, \hat{J}) = \frac{2}{p(p-1)} \sum_{i < j} (\hat{J}_{ij} - J_{ij})^2$.

For each underlying graph presented in Section 4.1.2, we generate datasets with 200 observations where the dimension of binary variables varies from 18 to 34. Then, we apply our methods and the competitor on these datasets according to details settings shown in the supplementary material. The simulation results based on 100 random replications are demonstrated in Figure 3. From the exhibited comparison, we can see that, compared to the state-of-the-art methods with ℓ_1 regularization, SIMPLE has a very competitive TPR, but it also would have a significantly lower FPR, which leads to its MCC, a measure that shows overall structure learning performance, would be higher than that of other approaches. Thus, from the perspective of graph support recovery, SIMPLE outperforms other methods under the high-dimensional setting. The high false inclusion is not surprising because the biases caused by the ℓ_1 penalty force the models to include more edges for compensation (Fan and Li, 2001; Xue et al., 2012).

On the other hand, in terms of MSE, it is obvious that MSE generally increases as the dimension gets higher, whatever method is implemented, and the result may be due to a faster increase in MSE than in dimension. What’s more, SIMPLE also owns the best performance in parameter estimation. The outstanding parameter estimation comes from the unbiasedness of the ℓ_0 constraint that only encourages sparsity but does not shrink the estimation. Therefore, we can conclude that SIMPLE owns outstanding performance and can provide a good estimator in the high-dimensional regime.

4.3 Runtime analysis

Adopting the numerical settings in Section 4.2, we further investigate the computational performance in these cases. As shown in Figure 4, the SIMPLE demonstrates the fastest performance among the five benchmarked Ising models. Remarkably, the computational advantage is tremendous, with up to a 100-fold speedup compared to other methods. Furthermore, experiments across these various models reveal a consistent pattern of computational efficiency: SIMPLE is the fastest method, followed by logRISE, RISE, and finally RPLE method. The results in Figure 4 refute the widely held belief that the best-subset selection approach is not feasible for learning high-dimensional Ising models. More importantly, the fitted curves (displayed in the top-left corner of each panel) depicting dimensionality against computation time show that the runtime of SIMPLE scales quadratically with respect to p . This confirms the computational complexity of SIMPLE is polynomial.

5 US Senate Voting Data Analysis

How humans interact with each other is one of the most important problems in social science (Shneiderman, 2008; Lazer et al., 2009). In the current and extremely divisive political environment in the U.S. and the world, it is more important than ever to study how individuals, including politicians, behave; for example, how politicians vote (Shneiderman, 2008), and why bipartisanship occurs when it is extremely unpopular and politically risky within the base of their party. Studying social interactions, however, is challenging because we cannot see people’s inner thoughts. Reconstructing the hidden information from observable individual behaviors, such as politicians’ voting records, is thus critically vital but also highly difficult. Ising model reconstruction is a fundamental tool in sociology for this

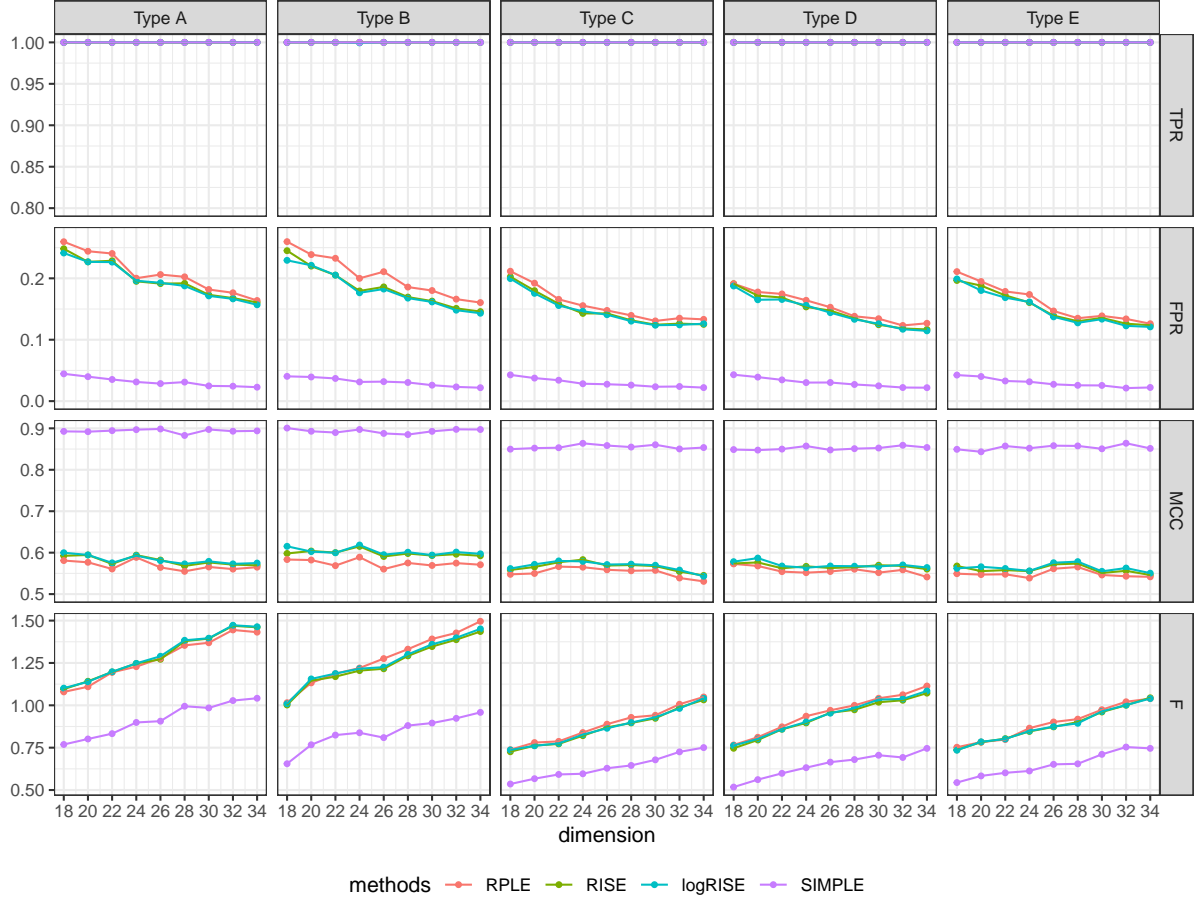


Figure 3: Structure recovery and parameter estimation performance comparison of the competing methods under high-dimensional settings.

purpose.

The US Senate Congress Voting Dataset is a popular test case for Ising model reconstruction. We consider data from the 112th to the 117th Congresses that are fetched from the VoteView (Lewis et al., 2019). The Senate votes “Yea” or “Nay” on federal legislation that affects all aspects of US domestic and foreign policy. If a vote is missing, it is imputed as “Nay” (Banerjee et al., 2008). Binary variables can be used to describe senators’ votes. For each Congress, an Ising model can be built to shed light on senators’ interactions with one another (see Figure 5). The senators can be loosely classified into two groups in this

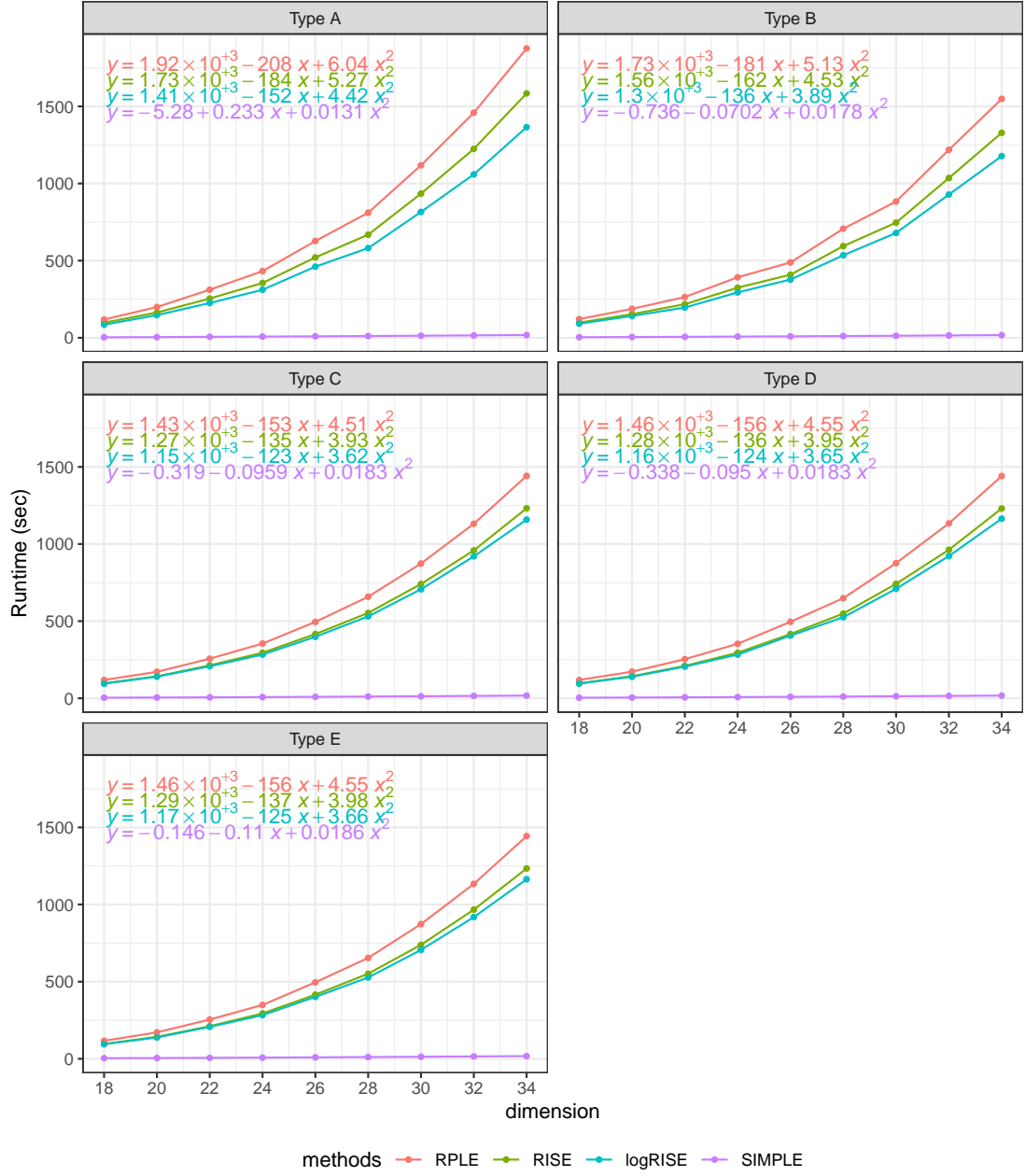


Figure 4: The dimension versus runtime scatterplot under high-dimensional settings.

figure: the Republicans and the Democrats. In line with both common sense and prior research of Banerjee et al. (2008) in just one Congress, it stands to reason that those within a party will have a stronger bond with one another than those from opposing parties. From

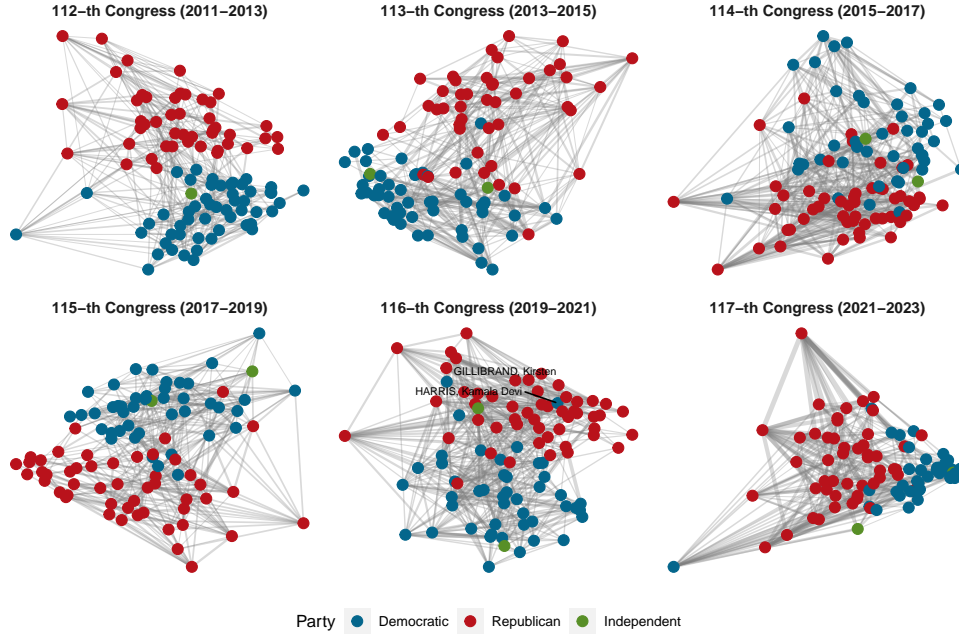


Figure 5: Voting records from the 112th to 117th Congresses are estimated by the SIMPLE for the US Senate. The SIMPLE uses the first two eigenvectors of the estimated interaction matrix to determine the node layout. The numbers of senators in the six Congresses are: 99, 98, 100, 96, 98, 97, respectively. Only senators who have neighbors are shown.

Figure 5, the 112th and 117th Congresses were visually more distinct. The 112th Congress had a greater degree of partisanship than any other. The Washington Post (Matthews, 2013) reported that the 112th Congress was the most polarized ever as measured by the DW-NOMINATE score (Poole and Rosenthal, 1985). We apply the spectral clustering method (Shi and Malik, 2000) on the reconstructed Ising model to make predictions, and get an unsupervised classifier with an accuracy rate of nearly 90%. Next, the Democratic senators in the 117th Congress displayed the most concentrated and out-of-the-ordinary pattern. This Senate is made up of 50 Republicans, 48 Democrats, and 2 Independents

who caucus with the Democrats. This makes the Senate effectively evenly split, only the third time in US history. Without any leeway for dissent, to support the agendas of the Democrat president, the Democrats need to be fully united (Rakich, 2021).

On a micro level, the political intention of the senators can be investigated from estimated networks and important insights can be unearthed. For example, in the 116th Congress, the voting pattern of two Democrat senators, Kamala Harris and Kirsten Gillibrand, had voted with the Republican Party. Although there is no particularly media attention for the fact that the current vice president sometimes agreed with the Republicans, her fellow senator Gillibrand (Gillibrand, 2021), who worked together with her during the 2019 Democratic presidential primary debate (Herman, 2019), was known to once hold conservative political views (Merica, 2019). The estimated interaction of 0.57 between these leaders may suggest that the vice president might be more conservative than the public is informed.

6 Conclusion and Discussion

Finding the optimal sample complexity solution for the reconstruction of the Ising model is an open problem that is explored in this study. We introduce the SIMPLE approach, and from theory and computation, shows that it is provable global. Moreover, it can be solved with polynomial complexity under realistic conditions. To the best of our knowledge, it is the first known approach that reaches the global optimality in a polynomial time. This means that our method can reconstruct various Ising models, even challenging models with low temperature and hubs, where existing methods require a larger sample complexity. Evidence from the real-world example also suggests that the SIMPLE can recover the interactions of complex systems and shed light on subtle information from apparently

opaque observations.

More efforts are deserves to enlarge the impact of sparse learning approach and the algorithm for solving. For example, one promising direction is extending our approach to recover Potts models for discrete variables (Wu, 1982; Zhu et al., 2023). From application, our solution facilitates the new findings on cutting-edge scientific problems such as functional connectome and disease connectome.

References

- Banerjee, O., L. E. Ghaoui, and A. d’Aspremont (2008). Model selection through sparse maximum likelihood estimation for multivariate gaussian or binary data. *Journal of Machine Learning Research* 9(Mar), 485–516.
- Barabási, A.-L. (2009). Scale-free networks: a decade and beyond. *Science* 325(5939), 412–413.
- Battiston, S., J. D. Farmer, A. Flache, D. Garlaschelli, A. G. Haldane, H. Heesterbeek, C. Hommes, C. Jaeger, R. May, and M. Scheffer (2016, February). Complexity theory and financial regulation. *Science* 351(6275), 818–819.
- Besag, J. (1975). Statistical analysis of non-lattice data. *Journal of the Royal Statistical Society: Series D (The Statistician)* 24(3), 179–195.
- Chow, C. and C. Liu (1968). Approximating discrete probability distributions with dependence trees. *IEEE transactions on Information Theory* 14(3), 462–467.
- Cocco, S., S. Leibler, and R. Monasson (2009, August). Neuronal couplings between retinal

- ganglion cells inferred by efficient inverse statistical physics methods. *Proceedings of the National Academy of Sciences* 106(33), 14058–14062.
- Decelle, A. and F. Ricci-Tersenghi (2014, February). Pseudolikelihood decimation algorithm improving the inference of the interaction network in a general class of ising models. *Physical Review Letters* 112(7), 070603.
- Dedieu, A., M. Lázaro-Gredilla, and D. George (2021). Sample-efficient l0-l2 constrained structure learning of sparse ising models. In *Proceedings of the AAAI Conference on Artificial Intelligence*, Volume 35, pp. 7193–7200.
- Fan, J. and R. Li (2001). Variable selection via nonconcave penalized likelihood and its oracle properties. *Journal of the American Statistical Association* 96(456), 1348–1360.
- Fan, Y. and C. Y. Tang (2013). Tuning parameter selection in high dimensional penalized likelihood. *Journal of the Royal Statistical Society: Series B (Statistical Methodology)* 75(3), 531–552.
- Geyer, C. J. (1994). On the convergence of monte carlo maximum likelihood calculations. *Journal of the Royal Statistical Society: Series B (Methodological)* 56(1), 261–274.
- Gillibrand, K. (2021, August). One year ago today, joe Biden chose kamalaharris to be his vice president. and every single day, my friend is making america so proud. <https://twitter.com/sengillibrand/status/1425567127696777216>.
- Grabowski, A. (2009). Opinion formation in a social network: The role of human activity. *Physica A: Statistical Mechanics and its Applications* 388(6), 961–966.
- Herman, L. (2019, August). The women worked together in last night’s debate. this

- race could use more of that. <https://www.refinery29.com/en-us/2019/08/239485/kamala-harris-kirsten-gillibrand-democratic-debate-joe-biden-op-ed>.
- Höfling, H. and R. Tibshirani (2009). Estimation of sparse binary pairwise markov networks using pseudo-likelihoods. *Journal of Machine Learning Research* 10(Apr), 883–906.
- Huang, J., Y. Jiao, Y. Liu, and X. Lu (2018). A constructive approach to l_0 penalized regression. *Journal of Machine Learning Research* 19(1), 403–439.
- Jalali, A., C. Johnson, and P. Ravikumar (2011). On learning discrete graphical models using greedy methods. *Advances in Neural Information Processing Systems* 24.
- Kappen, H. and F. de Borja Rodríguez Ortiz (1997). Boltzmann machine learning using mean field theory and linear response correction. *Advances in neural information processing systems* 10.
- Kunkin, W. and H. L. Frisch (1969, January). Inverse problem in classical statistical mechanics. *Physical Review* 177(1), 282–287.
- Lazer, D., A. Pentland, L. Adamic, S. Aral, A.-L. Barabási, D. Brewer, N. Christakis, N. Contractor, J. Fowler, M. Gutmann, T. Jebara, G. King, M. Macy, D. Roy, and M. Van Alstyne (2009, February). Computational social science. *Science* 323(5915), 721–723.
- Lewis, J. B., K. Poole, H. Rosenthal, A. Boche, A. Rudkin, and L. Sonnet (2019). Voteview: Congressional roll-call votes database. <https://voteview.com/> (accessed 27 July 2018).
- Lokhov, A. Y., M. Vuffray, S. Misra, and M. Chertkov (2018). Optimal structure and parameter learning of ising models. *Science advances* 4(3), e1700791.

- Marinazzo, D., M. Pellicoro, G. Wu, L. Angelini, J. M. Cortés, and S. Stramaglia (2014, April). Information transfer and criticality in the ising model on the human connectome. *PLOS ONE* 9(4), e93616.
- Matthews, D. (2013, January). It’s official: The 112th congress was the most polarized ever. <https://www.washingtonpost.com/news/wonk/wp/2013/01/17/its-official-the-112th-congress-was-the-most-polarized-ever/>.
- Merica, D. (2019, January). Gillibrand doesn’t shy away from her conservative past in iowa. <https://edition.cnn.com/2019/01/20/politics/gillibrand-conservative-past-iowa-democrats/index.html>.
- Miasojedow, B. and W. Rejchel (2018). Sparse estimation in ising model via penalized monte carlo methods. *Journal of Machine Learning Research* 19(1), 2979–3004.
- Montanari, A. and J. Pereira (2009). Which graphical models are difficult to learn? *Advances in Neural Information Processing Systems* 22.
- Nguyen, H. C. and J. Berg (2012, August). Mean-field theory for the inverse ising problem at low temperatures. *Physical Review Letters* 109(5), 050602.
- Nguyen, H. C., R. Zecchina, and J. Berg (2017). Inverse statistical problems: from the inverse ising problem to data science. *Advances in Physics* 66(3), 197–261.
- Noble, A. E., T. S. Rosenstock, P. H. Brown, J. Machta, and A. Hastings (2018, February). Spatial patterns of tree yield explained by endogenous forces through a correspondence between the ising model and ecology. *Proceedings of the National Academy of Sciences* 115(8), 1825–1830.

- Poole, K. T. and H. Rosenthal (1985). A spatial model for legislative roll call analysis. *American Journal of Political Science* 29(2), 357–384.
- Rakich, N. (2021, September). Why house democrats may be more united than they seem. <https://fivethirtyeight.com/features/why-house-democrats-may-be-more-united-than-they-seem/>.
- Raskutti, G., M. J. Wainwright, and B. Yu (2011). Minimax rates of estimation for high-dimensional linear regression over ℓ_q -balls. *IEEE transactions on information theory* 57(10), 6976–6994.
- Ravikumar, P., M. J. Wainwright, J. D. Lafferty, et al. (2010). High-dimensional ising model selection using l_1 -regularized logistic regression. *Annals of Statistics* 38(3), 1287–1319.
- Rigollet, P. (2012). Kullback-leibler aggregation and misspecified generalized linear models. *Annals of Statistics* 40(2), 639–665.
- Santhanam, N. P. and M. J. Wainwright (2012). Information-theoretic limits of selecting binary graphical models in high dimensions. *IEEE Transactions on Information Theory* 58(7), 4117–4134.
- Sara van de Geer and Peter Bühlmann (2013, April). ℓ_0 -penalized maximum likelihood for sparse directed acyclic graphs. *Annals of Statistics* 41(2), 536–567.
- Saremi, S. and T. J. Sejnowski (2013, February). Hierarchical model of natural images and the origin of scale invariance. *Proceedings of the National Academy of Sciences* 110(8), 3071–3076.
- Shi, J. and J. Malik (2000). Normalized cuts and image segmentation. *IEEE Transactions on pattern analysis and machine intelligence* 22(8), 888–905.

- Shneiderman, B. (2008, March). Science 2.0. *Science* 319(5868), 1349–1350.
- Vuffray, M., S. Misra, A. Lokhov, and M. Chertkov (2016). Interaction screening: Efficient and sample-optimal learning of ising models. *Advances in Neural Information Processing Systems* 29, 2595–2603.
- Weistuch, C., L. R. Mujica-Parodi, R. M. Razban, B. Antal, H. van Nieuwenhuizen, A. Amgalan, and K. A. Dill (2021, October). Metabolism modulates network synchrony in the aging brain. *Proceedings of the National Academy of Sciences* 118(40), e2025727118.
- Wu, F.-Y. (1982). The potts model. *Reviews of modern physics* 54(1), 235.
- Xue, L., H. Zou, T. Cai, et al. (2012). Nonconcave penalized composite conditional likelihood estimation of sparse ising models. *Annals of Statistics* 40(3), 1403–1429.
- Zhang, Y., J. Zhu, J. Zhu, and X. Wang (2023). A splicing approach to best subset of groups selection. *INFORMS Journal on Computing* 35(1), 104–119.
- Zhu, J., L. Hu, J. Huang, K. Jiang, Y. Zhang, S. Lin, J. Zhu, and X. Wang (2022). abess: A fast best subset selection library in Python and R. *Journal of Machine Learning Research*.
- Zhu, J., C. Wen, J. Zhu, H. Zhang, and X. Wang (2020). A polynomial algorithm for best-subset selection problem. *Proceedings of the National Academy of Sciences* 117(52), 33117–33123.
- Zhu, J., J. Zhu, B. Tang, X. Chen, H. Lin, and X. Wang (2023). Best-subset selection in generalized linear models: A fast and consistent algorithm via splicing technique. *arXiv preprint arXiv:2308.00251*.